

Title: How do biological traits affect brachiopod taxonomic
2 survival? A hierarchical Bayesian approach.

Running title: How do biological traits affect taxonomic survival?

4 **Author:** Peter D Smits, psmits@uchicago.edu, Committee on Evolutionary
Biology, University of Chicago

6 **Keywords:** extinction, macroevolution, macroecology, Paleozoic, selection

Word count: ?

8 **Table count:** 0

Figure count: ?

10 **Data archival location:** Dryad?

Abstract

12 How does ecology affect taxon duration? While the effect of
geographic range on extinction risk is well documented, the effects of
14 other traits are less well documented. Here, I analyze patterns of
Paleozoic brachiopod genus durations and how various biological traits
16 are related to systematic differences in expected extinction risk. I analyze
geographic range, affinity for epicontinental seas versus open ocean
18 environments, and body size. Additionally, I allow for environmental
affinity to have a nonlinear effect on duration. I do this in a hierarchical
20 Bayesian modeling context, allowing me to model the possible interaction
between the effects of biological traits and time of origination. I find weak
22 that as extinction risk increases, the expected strength of the selection
gradient on biological traits (except body size) increases. This manifests
24 as greater expected differences in extinction risk for each unit change in
geographic range and environmental preference during periods of high
26 extinction risk, while a much flatter expected selection gradient during
periods of low extinction risk. I find evidence for a nonlinear relationship
28 between environmental preference and extinction risk such that
intermediate affinities (“generalists”) have a lower expected extinction
30 risk than either end members (“specialists”). Interestingly, I find that as
extinction risk increases, the peakedness of this relationship is expected to
32 increase as well. These results demonstrate the importance of directly
modeling the structure inherent in the observed data as a means to better
34 understand which processes may have been driving the observed patterns
of diversification.

1 Introduction

How do biological traits affect extinction risk? Jablonski (1986) observed that during periods of high expected extinction risk, the effects of biological traits on survival decreased in importance. However, this pattern was weakest/absent in the effect of geographic range on survival (Jablonski, 1986). Biological traits are defined here as descriptors of a taxon’s adaptive zone, which is the set of biotic–biotic and biotic–abiotic interactions that a taxon can experience. In effect, these are descriptors of a taxon’s broad-sense ecology.

Jablonski (1986) phrased their conclusions in terms of background versus mass extinction, but this scenario is readily transferable to a continuous variation framework as there is no obvious distinction in terms of extinction rate between these two states (Wang, 2003). I adopt a continuous variation framework as this is more amenable for modeling the relationship between taxon traits and extinction risk. Additionally, the Jablonski (1986) scenario has strong model structure requirements in order to test its proposed macroevolutionary mechanism. Not only do the taxon trait effects need to be modeled, but the relationships between these effects need to be modeled as well.

Two possible macroevolutionary mechanisms which may underly the pattern observed by Jablonski (1986) are: the effect of geographic range on predictive survival remains constant and those of other biological traits decrease, and the effect of geographic range in predicting survival increases and those of other biological traits stay constant.

I model taxon durations because trait based differences in extinction risk should manifest as differences in taxon durations. Namely, a species with a beneficial trait should survive longer, on average, than a species without that beneficial trait. Conceptually, taxon survival can be considered an aspect of “taxon fitness”

62 along with expected lineage branching/origination rate (Cooper, 1984, Palmer
and Feldman, 2012). The analysis of taxon durations, or time from origination
64 to extinction, falls under the purview of survival analysis, a field of applied
statistics commonly used in health care (Klein and Moeschberger, 2003) but has
66 a long history in paleontology (Simpson, 1944, 1953, Van Valen, 1973, 1979).

Geographic range is widely considered the most important taxon trait for
68 estimating differences in extinction risk at nearly all times with large geographic
range associated with low extinction risk (Jablonski, 1986, 1987, Jablonski and
70 Roy, 2003, Payne and Finnegan, 2007). I expect this to hold true nearly always.

Miller and Foote (2009) demonstrated that during several mass extinctions taxa
72 associated with open ocean environments tend to have a greater extinction risk
than those taxa associated with epicontinental seas. During periods of
74 background extinction, however, they found no consistent difference between
taxa favoring either environment. Because of this study, the following prediction
76 for survival patterns can be made: as extinction risk increases, taxa associated
with open ocean environments should generally increase in extinction risk versus
78 those that favor epicontinental seas.

There is also a possible nonlinear relationship between environmental preference
80 and taxon duration. A long standing hypothesis is that generalists or
unspecialized taxa will have greater survival than specialists (Baumiller, 1993,
82 Liow, 2004, 2007, Nürnberg and Aberhan, 2013, 2015, Simpson, 1944) SMITS,
IN PREP. I allowed for environmental preference to possibly have a parabolic
84 effect on species duration

Body size, measured as shell length (Payne et al., 2014), was also considered as
86 a potentially informative covariate. Body size is a proxy for metabolic activity
and other, correlated, life history traits (Payne et al., 2014). There is no strong

88 hypothesis of how body size effects extinction risk in brachiopods, meaning a
positive, negative, or null effect are all plausible.

90 I adopt a hierarchical Bayesian survival modeling approach, which represents a
conceptual and statistical unification of the paleontological dynamic and cohort
92 survival analytic approaches (Baumiller, 1993, Foote, 1988, Raup, 1975, 1978,
Simpson, 2006, Van Valen, 1973, 1979). By using a Bayesian framework I am
94 able to quantify the uncertainty inherent in the estimates of the effects of
biological traits on survival, especially in cases where the covariates of interest
96 (biological traits) are themselves known with error.

2 Materials and Methods

98 2.1 Analytical approach

Hierarchical modelling, sometimes called “mixed-effects modeling,” is a
100 statistical approach which explicitly takes into account the structure of the
observed data in order to model both the within and between group variance
102 (Gelman et al., 2013, Gelman and Hill, 2007). The units of study (e.g. genera)
each belong to a single grouping (e.g. origination cohort). These groups are
104 considered draws from a shared probability distribution (e.g. all cohorts,
observed and unobserved). The group-level parameters are then estimated
106 simultaneously as the other parameters of interest (e.g. covariate effects)
(Gelman et al., 2013). The subsequent estimates are partially pooled together,
108 where parameters from groups with large samples or effects remain large while
those of groups with small samples or effects are pulled towards the overall
110 group mean.

This partial pooling is one of the greatest advantages of hierarchical modeling.

112 By letting the groups “support” each other, parameter estimates then better
reflect our statistical uncertainty. Additionally, this partial pooling helps control
114 for multiple comparisons and possibly spurious results as effects with little
support are drawn towards the overall group mean (Gelman et al., 2013,
116 Gelman and Hill, 2007).

All covariate effects (regression coefficients), as well as the intercept term
118 (baseline extinction risk), were allowed to vary by group (origination cohort).
The covariance/correlation between covariate effects was also modeled. This
120 hierarchical structure allows inference for how covariates effects may change
with respect to each other while simultaneously estimating the effects
122 themselves, propagating our uncertainty through all estimates.

Additionally, instead of relying on point estimates of environmental affinity, I
124 treat environmental affinity as a continuous measure of the difference between
the taxon’s environmental occurrence pattern and the background occurrence
126 pattern (Appendix A).

2.2 Fossil occurrence information

128 The dataset analyzed here is derived from the a combination of the occurrence
information from Foote and Miller (2013) and the body size data from Payne
130 et al. (2014). The Foote and Miller (2013) dataset is based on the Paleobiology
Database (<http://www.paleodb.org>); see Foote and Miller (2013) for a full
132 description of the inclusion criterion. Additionally, epicontinental versus open
ocean assignemnts for occurrence information are based on Miller and Foote
134 (2009). NOTE: I DON’T KNOW HOW THIS MAY NEED TO BE UPDATED.

Sampled occurrences were restricted to those with paleolatitude and
136 paleolongitude coordinates, assignment to either epicontinental or open-ocean

environment, and belonging to a genus present in the body size dataset (Payne
 138 et al., 2014). Genus duration was calculated as the number of geologic stages
 from first appearance to last appearance, inclusive. Genera with a last
 140 occurrence in or after Changhsingian stage were right censored at the
 Changhsingian. Genera with a duration of only one stage were left censored
 142 (Appendix C). The covariates used to model genus duration were geographic
 range size (r), environmental preference (v, v^2), and body size (m).
 144 Geographic range was calculated using an occupancy approach. First, all
 occurrences were projected onto an equal-area cylindrical map projection. Each
 146 occurrence was then assigned to one of the cells from a 70×34 regular raster
 grid placed on the map. Each grid cell represents approximately 250,000 km².
 148 The map projection and regular lattice were made using shape files from
<http://www.naturalearthdata.com/> and the **raster** package for R (Hijmans,
 150 2015).

For each stage, the total number of occupied grid cells, or cells in which a fossil
 152 occurs, was calculated. Then, for each genus, the number of grid cells occupied
 by that genus was calculated. Dividing the genus occupancy by the total
 154 occupancy gives the relative occupancy of that genus. Mean relative genus
 occupancy was then calculated as the mean of the per stage relative occupancies
 156 of that genus.

Body size data was sourced directly from Payne et al. (2014). Because those
 158 measurements are presented without error, a measurement error model similar
 to the one for environmental affinity could not be implemented (Appendix A).

160 Prior to analysis, geographic range and body size were transformed and
 standardized in order to improve interpretability of the results. Geographic
 162 range, which can only vary between 0 and 1, was logit transformed. Body size,

which is defined for all positive real values, was natural log transformed. These
164 covariates were then standardized by mean centering and dividing by two times
their standard deviation following Gelman and Hill (2007).

166 **2.3 Survival model**

Genus durations were modeled as time-till-event data (Klein and Moeschberger,
168 2003), with covariate information used in estimates of extinction risk as a
hierarchical regression model. Genus durations were assumed to follow either an
170 exponential or Weibull distribution. Each of these distributions makes
assumptions about how duration may effect extinction risk (Klein and
172 Moeschberger, 2003). The exponential distribution assumes that extinction risk
is independent of duration. In contrast, the Weibull distribution allows for age
174 dependent extinction via the shape parameter α , though only as a monotonic
function of duration. Importantly, the Weibull distribution is equivalent to the
176 exponential distribution when $\alpha = 1$.

The following variables are defined: y_i is the duration of genus i in geologic
178 stages, X is the matrix of covariates including a constant term, B_j is the vector
of regression coefficients for origination cohort j , Σ is the covariance matrix of
180 the regression coefficients, τ is the vector of scales the standard deviations of
the between-cohort variation in regression coefficient estimates, and Ω is the
182 correlation matrix of the regression coefficients.

The exponential model is defined

$$\begin{aligned}
y_i &\sim \text{Exponential}(\lambda) \\
\lambda_i &= \exp(\mathbf{X}_i B_{j[i]}) \\
B &\sim \text{MVN}(\vec{\mu}, \Sigma) \\
\Sigma &= \text{Diag}(\vec{\tau}) \Omega \text{Diag}(\vec{\tau}) \\
\mu_\kappa &\sim \begin{cases} \mathcal{N}(0, 5) & \text{if } k \neq r, \text{ or} \\ \mathcal{N}(-1, 1) & \text{if } k = r \end{cases} \\
\tau_\kappa &\sim \text{C}^+(1) \text{ for } \kappa \in 1 : k \\
\Omega &\sim \text{LKJ}(2).
\end{aligned} \tag{1}$$

184 Similarly, the Weibull model is defined

$$\begin{aligned}
y_i &\sim \text{Weibull}(\alpha, \sigma) \\
\sigma_i &= \exp\left(\frac{-(\mathbf{X}_i B_{j[i]})}{\alpha}\right) \\
B &\sim \text{MVN}(\vec{\mu}, \Sigma) \\
\Sigma &= \text{Diag}(\vec{\tau}) \Omega \text{Diag}(\vec{\tau}) \\
\alpha &\sim \text{C}^+(2) \\
\mu_k &\sim \begin{cases} \mathcal{N}(0, 5) & \text{if } k \neq r, \text{ or} \\ \mathcal{N}(-1, 1) & \text{if } k = r \end{cases} \\
\tau_k &\sim \text{C}^+(1) \\
\Omega &\sim \text{LKJ}(2).
\end{aligned} \tag{2}$$

The principle difference between this model and the previous (Eq. 1) is the

186 inclusion of the shape parameter α . Note that σ is approximately equivalent to

1/ λ .

188 For an explanation of how this model was developed and parameter
explanations, please see Appendix B. Note that these models (Eq. 1, 2) do not
190 include how the uncertainty in environmental affinity is included nor how
censored observations are included. For an explanation of both of these aspects,
192 see Appendices A and C.

2.4 Parameter estimation

194 The joint posterior was approximated using a Markov-chain Monte Carlo
routine that is a variant of Hamiltonian Monte Carlo called the No-U-Turn
196 Sampler (Hoffman and Gelman, 2014) as implemented in the probabilistic
programming language Stan (Stan Development Team, 2014a). The posterior
198 distribution was approximated from four parallel chains run for 10,000 draws
each, split half warm-up and half sampling and thinned to every 10th sample for
200 a total of 5000 posterior samples. Chain convergence was assessed via the scale
reduction factor \hat{R} where values close to 1 ($\hat{R} < 1.1$) indicate approximate
202 convergence. Convergence means that the chains are approximately stationary
and the samples are well mixed (Gelman et al., 2013).

2.5 Model evaluation

Models were evaluated using both posterior predictive checks and an estimate of
206 out-of-sample predictive accuracy. The motivation behind posterior predictive
checks as tools for determining model adequacy is that replicated data sets
208 using the fitted model should be similar to the original data (Gelman et al.,
2013). Systematic differences between the simulations and observations indicate

210 weaknesses of the model fit. An example of a technique that is very similar
would be inspecting the residuals from a linear regression.

212 The strategy behind posterior predictive checks is to draw simulated values
from the joint posterior predictive distribution, $p(y^{rep}|y)$, and then compare
214 those draws to the empirically observed values (Gelman et al., 2013). To
accomplish this, for each replicate, a single value is drawn from the marginal
216 posterior distributions of each regression coefficient from the final model as well
as α for the Weibull model (Eq. 1, 2). Then, given the covariate information \mathbf{X} ,
218 a new set of n genus durations are generated giving a single replicated data set
 y^{rep} . This is repeated 1000 times in order to provide a distribution of possible
220 values that could have been observed given the model.

In order to compare the fitted model to the observed data, various graphical
222 comparisons or test quantities need to be defined. The principal comparison
used here is a comparison between non-parameteric approximation of the
224 survival function $S(t)$ as estimated from both the observed data and each of the
replicated data sets. The purpose of this comparison is to determine if the
226 model approximates the same survival/extinction pattern as the original data.

The exponential and Weibull models were compared for out-of-sample predictive
228 accuracy using the widely-applicable information criterion (WAIC) (Watanabe,
2010). Out-of-sample predictive accuracy is a measure of the expected fit of the
230 model to new data. However, because the Weibull model reduces to the
exponential model when $\alpha = 1$ my interest is not in choosing between these
232 models. Instead, comparisons of WAIC values are useful for better
understanding the effect of model complexity on out-of-sample predictive
234 accuracy. The calculation of WAIC used here corresponds to the “WAIC 2”
formulation recommended by Gelman et al. (2013). For an explanation of how
236 WAIC is calculated, see Appendix D. Lower values of WAIC indicate greater

expected out-of-sample predictive accuracy than higher values.

3 Results

As stated above, posterior approximations for both the exponential and Weibull models achieved approximate stationarity after 10,000 steps, as all parameter estimates have an $\hat{R} < 1.1$.

Comparisons of the survival functions estimated from 1000 posterior predictive data sets to the estimated survival function of the observed genera demonstrates that both the exponential and Weibull models approximately capture the observed pattern of extinction (Fig. 1). The major difference in fit between the two models is that the Weibull model has a slightly better fit for longer lived taxa than the exponential model.

Additionally, the Weibull model is expected to have slightly better out-of-sample predictive accuracy when compared to the exponential model (WAIC 4577 versus 4605, respectively). 1). Because the difference in WAIC between these two models is large, while results from both the exponential and Weibull models will be presented, only those from the Weibull model will be discussed.

Estimates of the overall mean covariate effects μ can be considered time-invariant generalizations for brachiopod survival during the Paleozoic SMITS IN PREP (Fig. 2). Consistent with prior expectations, geographic range size has a negative effect on extinction risk, where genera with large ranges having greater durations than genera with small ranges.

I find that there is an approximately 93% posterior probability that the overall effect of increasing body size decreases expected extinction risk. This parameter, however, is not very large and is within two standard deviations of 0 (mean

$\mu_m = -0.15$, standard deviation 0.1). Because of this, I interpret this as weak
 262 evidence for increases in body size to be associated with a decrease in expected
 extinction risk.

264 Interpretation of the effect of environmental preference v on duration is slightly
 more involved. Because a quadratic term is the equivalent of an interaction
 266 term, both μ_v and μ_{v^2} have to be interpreted together because it is illogical to
 change values of v without also changing values v^2 . To determine the nature of
 268 the effect of v on duration I calculated the multiplicative effect of environmental
 preference on extinction risk.

270 Given mean estimated extinction risk $\tilde{\sigma}$, we can define the extinction risk
 multiplier of an observation with environmental preference v_i as

$$\frac{\tilde{\sigma}_i}{\tilde{\sigma}} = f(v_i) = \exp\left(\frac{-(\mu_v v_i + \mu_{v^2} v_i^2)}{\alpha}\right). \quad (3)$$

272 This function $f(v_i)$ has a y-intercept of $\exp(0)$ or 1 because it does not have a
 non-zero intercept term. Equation 3 can be either concave up or down. A
 274 concave down $f(v_i)$ may indicate that genera of intermediate environmental
 preference have greater durations than either extreme, and *vice versa* for
 276 concave up function.

The expected effect of environmental preference as a multiplier of expected
 278 extinction risk can then be visualized (Fig. 3). This figure depicts 1000 posterior
 predictive estimates of Eq. 3 across all possible values of v . The number
 280 indicates the posterior probability that the function is concave down, with
 generalists having lower extinction risk/greater duration than either type of
 282 specialist. Note that the inflection point/optimum of Fig. 3 is approximately
 $x = 0$, something that is expected given the estimate of μ_v (Fig. 2).

284 The matrix Σ describing the covariance between the different coefficients

describes how these coefficients might vary together across the origination
 cohorts. Similar to how this was modeled (Eq. 1, 2), for interpretation purposes
 Σ can be decomposed into a vector of standard deviations $\vec{\tau}$ and a correlation
 matrix Ω .

The estimates of the standard deviation of between-cohort coefficient estimates
 τ indicate that some effects can vary greatly between-cohorts (Fig. 4).

Coefficients with greater values of τ have greater between-cohort variation. The
 covariate effects with the greatest between origination cohort variation are β_r ,
 β_v , and β_{v^2} . Estimates of β_m have negligible between cohort variation, as there
 is less between cohort variation than the between cohort variation in baseline
 extinction risk β_0 . However the amount of between cohort variation in estimates
 of β_{v^2} means that it is possible for the function describing the effect of
 environmental affinity to be upward facing for some cohorts (Eq. 3), which
 corresponds to environmental generalists being shorted lived than specialists in
 that cohort.

The correlation terms of Ω (Fig. 5) describe the relationship between the
 coefficients and how their estimates may vary together across cohorts. The
 correlations between the intercept term β_0 and the effects of the taxon traits are
 of particular interest for evaluating the Jablonski (1986) scenario (Fig. 5 first
 column/last row). Keep in mind that when β_0 is low, extinction risk is low; and
 conversely, when β_0 is high, then extinction risk is high.

Marginal posterior probabilities of the correlations between the level of baseline
 extinction risk β_0 and the effects of the taxon traits indicate that the correlation
 between expected extinction risk and both geographic range β_r and β_{v^2} are of
 particular note (Fig. 6).

There is approximately a 98% probability that β_0 and β_r are negatively

correlated (Fig. 6), meaning that as extinction risk increases, the
 312 effect/importance of geographic range on genus duration increases. This means
 that increases in baseline extinction rate are correlated with an increased
 314 importance of geographic range size. There is a 94% probability that β_0 and β_{v^2}
 are negatively correlated (Fig. 6), meaning that as extinction risk increases, the
 316 peakedness of $f(v_i)$ increases and the relationship tends towards concave down.
 Additionally, there is a 97% probability that values of β_r and β_{v^2} are positively
 318 correlated (Mean correlation 0.51, standard deviation 0.23).

While the overall group level estimates are of particular importance when
 320 defining time-invariant differences in extinction risk, it is also important and
 useful to analyze the individual level parameter estimates in order to better
 322 understand how parameters actually vary across cohorts.

In comparison to the overall mean extinction risk μ_0 , cohort level estimates β_0
 324 show some amount of variation through time as expected by estimates of τ_0
 (Fig. 7). A similar, if slightly greater, amount of variation is also observable in
 326 cohort estimates of the effect of geographic range β_r (Fig. 8). Again, smaller
 values of β_0 correspond to lower expected extinction risk. Similarly, smaller
 328 values of β_r correspond to greater decrease in extinction risk with increasing
 geographic range

330 How the effect of environmental affinity varies between cohorts can be observed
 by using the cohort specific coefficients estimates. Following the same procedure
 332 used earlier (Fig. 4), but substituting cohort specific estimates of β_v and β_{v^2} for
 μ_v and μ_{v^2} , the cohort specific effect of environmental preference as a multiplier
 334 of mean extinction risk can be calculated. This was done only for the Weibull
 model, though the observed pattern should be similar for the exponential model.
 336 As expected based on the estimates of τ_v and τ_{v^2} , there is greater variation in

the peakedness of $f(v_i)$ than there is variation between concave up and down
 338 functions (Fig. 9). 9 of the 33 cohorts have less than 50% posterior probability
 that generalists are potentially expected to be shorter lived than specialists,
 340 though two of those cases have approximately a 50% probability of being either
 concave up or down. This is congruent with the 0.86 posterior probability that
 342 $\mu_{v,2}$ is positive/ $f(v_i)$ is concave down.

Additionally, for some cohorts there is a quite striking pattern where the effect
 344 of environmental preference v has a nearly-linear relationship (Fig. 9). These are
 primarily scenarios where one of the end member preferences is expected to
 346 have a greater duration than either intermediate or the opposite end member
 preference. Whatever curvature is present in these nearly-linear cases is due to
 348 the definition of $f(v)$ as it is not defined for non-negative values of σ (Eq. 3). For
 most of the all stages between the Emsian through the Tournaisian, inclusive,
 350 intermediate preferences are of intermediate extinction risk when compared with
 epicontinental specialists (lowest risk) or open-ocean specialists (highest risk).
 352 This time period represents most of the Devonian.

4 Discussion

354 My results demonstrate that both the effects of geographic range and the
 peakedness/concavity of environmental preference are both negatively
 356 correlated with baseline extinction risk, meaning that as baseline extinction risk
 increases the effect sizes of both these traits are expected to increase (Fig. 6).
 358 This result supports neither of the two proposed macroevolutionary mechanisms
 for how biological traits should correlate with extinction risk. The observed
 360 correlation between the two effects as well as between the effects and baseline
 extinction risk instead implies that as baseline extinction risk increases, the

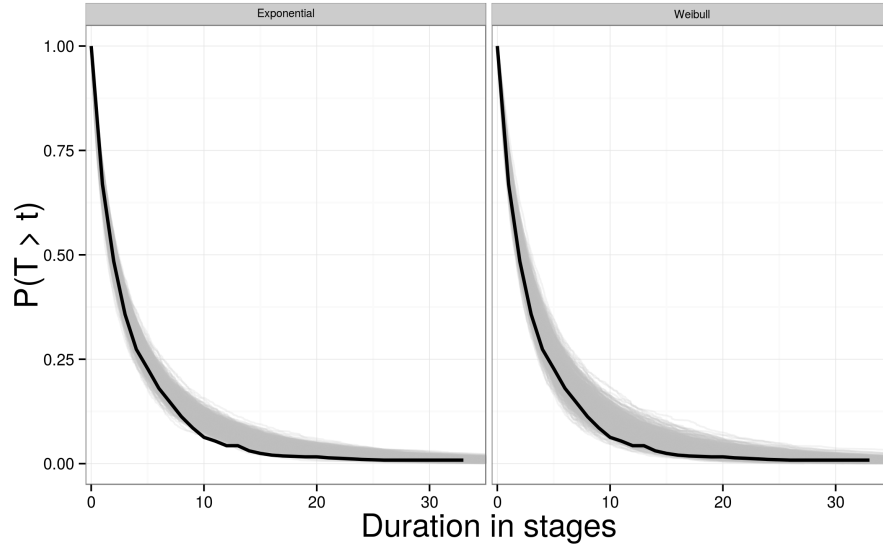


Figure 1: Comparison of empirical estimates of $S(t)$ versus estimates from 1000 posterior predictive data sets. $S(t)$ corresponds to $P(T > t)$ as it is the probability that a given genus observed at age t will continue to live. This is equivalent to the probability that t is less than the genus' ultimate duration T . Note that the Weibull (left) model has noticeably better fit to the data than the exponential (right).

362 strength of the total selection gradient on biological traits (except body size)
increases. This manifests as greater differences in extinction risk for each unit
364 difference in the biological covariates during periods of high extinction risk,
while a relatively flatter selection gradient during periods of low extinction risk.

366 There are two mass extinction events that are captured within the time frame
considered here: the Ordovician-Silurian and the Frasnian-Famennian. The
368 cohorts bracketing these events are worth considering in more detail.

The proposed mechanism for the end Ordovician mass extinction is a decrease
370 in sea level and the draining of epicontinental seas due to protracted glaciation
(Johnson, 1974, Sheehan, 2001). My results are broadly consistent with this
372 scenario with both epicontinental and open-ocean specialists having a much

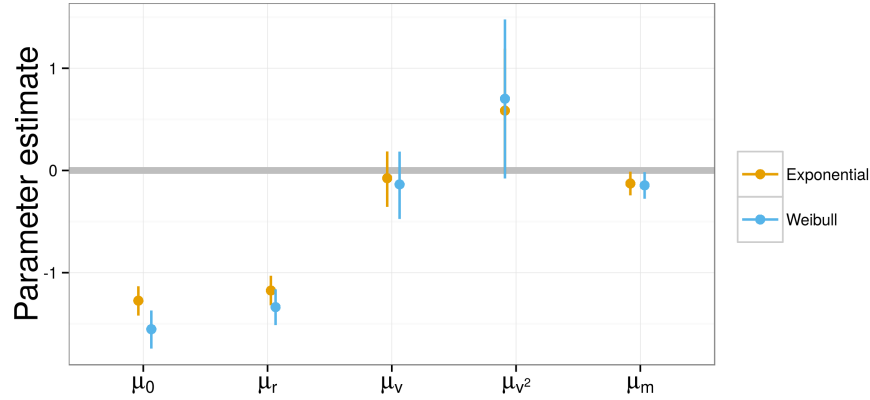


Figure 2: Estimates of the overall effects of the covariates on extinction risk. Included is also the estimate of μ_0 which corresponds to the intercept term or, because of standardization, the overall mean expected extinction risk. Estimates are presented for both the exponential (gold) and Weibull (blue) models. The point corresponds to the median of the posterior distribution, while the error bars correspond to the 80% credible intervals of the estimates.

lower expected duration than intermediate taxa (Fig. 9). All of the stages

374 between the Darriwillian and the Llandovery, except the Hirnantian, have a
greater than expected probability that $f(v)$ is concave down. The pattern for
376 the Darriwillian, which marks the supposed start of Ordovician glacial activity,
demonstrates that taxa tend to favor open-ocean environments are expected to
378 have a greater duration than either intermediate or epicontinental specialists, in
decreasing order.

380 For nearly the entire Devonian estimates of $f(v)$ indicate that one of the
environmental end members is favored over the other end member of
382 intermediate preference (Fig. 9). This is consistent with Miller and Foote (2009).
For the Givetian through the end of the Devonian and into the Tournaisian, I
384 find that epicontinental favoring taxa are expected to have a greater duration
than either intermediate or open-ocean specialists. Additionally, for nearly the

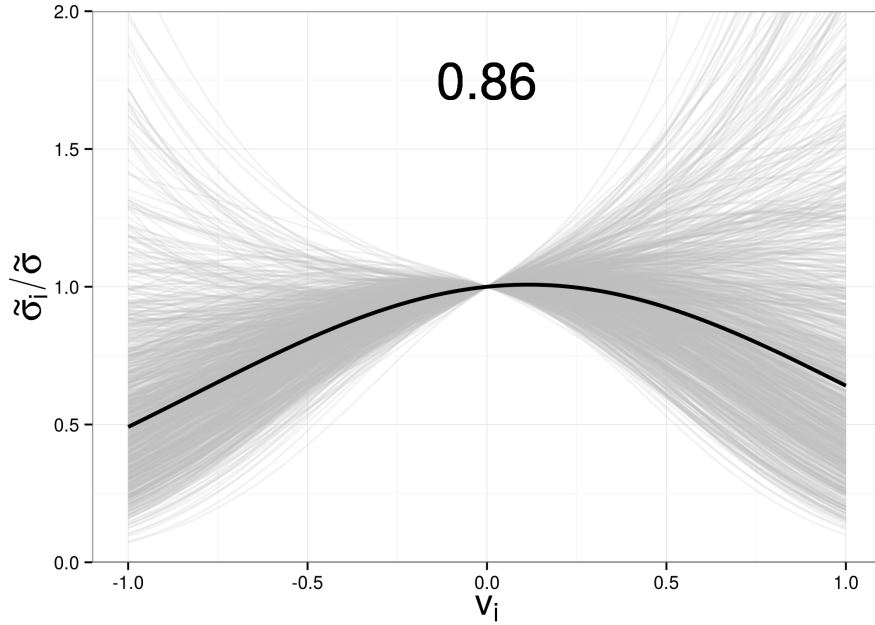


Figure 3: The overall expected relationship $f(v_i)$ between environmental affinity v_i and a multiplier of extinction risk (Eq. 3). Each grey line corresponds to a single draw from the posterior predictive distribution, while the black corresponds to the median of the posterior predictive distribution. The overall shape of $f(v_i)$ is concave down with an optimum of close 0, which corresponds to affinity approximately equal to the expectation based on background environmental occurrence rates.

entire Devonian except the Eifelian and through the Viséan, the cohort-specific estimates of $f(v)$ are concave-up. This is the opposite pattern than what is expected (Fig. 3). This result, however, seems to reflect the intensity of the seemingly nearly-linear difference in expected duration across the range of v) as opposed to an inversion of the weakly expected curvilinear pattern.

There is an approximate 86% posterior probability that taxa with intermediate environmental preferences are possibly expected to have a lesser extinction risk than either end members, the over all curvature of $f(v_i)$ is not very peaked, meaning that this relationship does not lead to very strong differences in

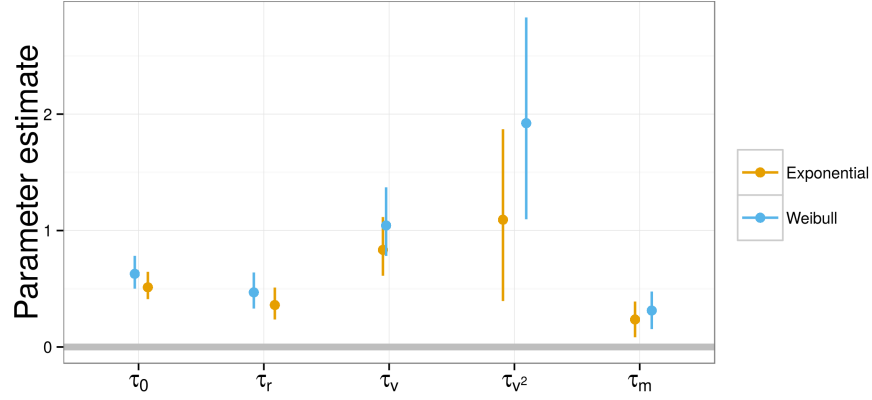


Figure 4: Estimates of the scale parameters describing the expected differences in the effect of the covariates, and of the intercept/baseline extinction risk, between cohorts. Higher values of τ correspond to greater expected differences between cohorts. Estimates are presented for both the exponential (gold) and Weibull (blue) models. The point corresponds to the median of the posterior distribution, while the error bars correspond to the 80% credible intervals of the estimates.

extinction risk (Fig. 3). This result gives weak support for the hypothesis that,
in general, environmental generalists survive for longer than environmental
specialists (Liow, 2004, 2007, Nürnberg and Aberhan, 2013, 2015, Simpson,
1944).

The variance in estimate of the overall $f(v_i)$ reflects the large between cohort
variance in cohort specific estimates of $f(v_i)$ (Fig. 9). Given that there is only a
86% posterior probability that the expected overall estimate of $f(v_i)$ is concave
down, it is not surprising that there are some stages where the theorized
relationship is in fact reversed. Additionally, as discussed earlier, some of those
same stages where $f(v_i)$ does not resemble the theorized nonlinear relation with
the optimum in the middle, but are instead is highly skewed or effectively linear
(Fig. 9).

These results do not necessarily refute “survival of the unspecialized” as a

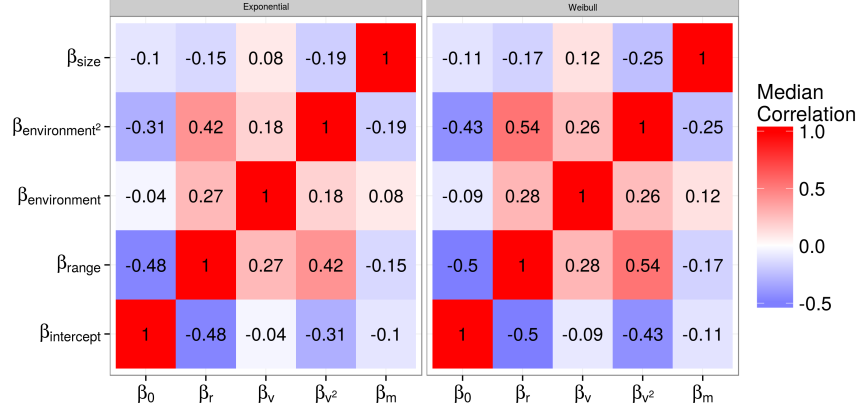


Figure 5: Heatmap for the median estimates of the terms of the correlation matrix Ω between cohort-level covariate effects. Both the exponential (left) and Weibull (right) models are presented. The off-diagonal terms are the correlation between the estimates of the cohort-level estimates of the effects of covariates, along with intercept/baseline extinction risk.

time-invariant generalization, but instead demonstrate how, while the expected group-level estimate of $f(v_i)$ might favor one hypothesis, there is still enough variability between cohorts so that in some realizations this pattern may not hold or can even be reversed. These results are also consistent with aspects of Miller and Foote (2009) who found that the effect of environmental preference on extinction risk was quite variable and without obvious patterning during times of background extinction.

This model can be improved through either increasing the number of analyzed taxon traits, expanding the hierarchical structure of the model to include other major taxonomic groups of interest, and the inclusion of explicit phylogenetic relationships between the taxa in the model as an additional hierarchical effect.

An example taxon trait that may be of particular interest is the affixing strategy or method of interaction with the substrate of the taxon. This trait has been found to be related to brachiopod survival (Alexander, 1977) so its

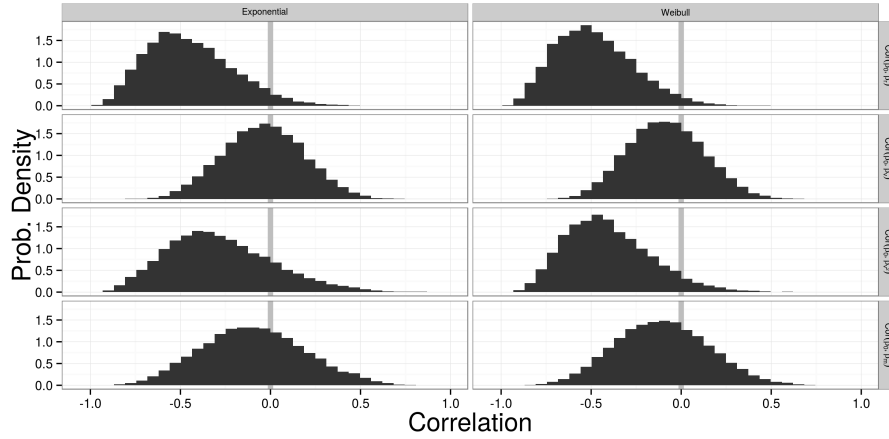


Figure 6: Marginal posterior distributions of the correlations between intercept terms/baseline extinction risk and the effects of each of the covariates. These are presented for both the exponential (left) and Weibull (right) models.

inclusion may be of particular interest.

It is theoretically possible to expand this model to allow for comparisons within and between major taxonomic groups. This approach would better constrain the brachiopod estimates while also allowing for estimation of similarities and differences in cross-taxonomic patterns. The major issue surrounding this particular expansion involves finding an similarly well sampled taxonomic group that is present during the Paleozoic. Example groups include Crinoidea, Ostracoda, and other “Paleozoic” groups (Sepkoski Jr., 1981).

Taxon traits like environmental preference or geographic range (Hunt et al., 2005, Jablonski, 1987) are most likely heritable, at least phylogenetically (Housworth et al., 2004, Lynch, 1991). Without phylogenetic context, this analysis assumes that differences in extinction risk between taxa are independent of those taxa’s shared evolutionary history (Felsenstein, 1985). In contrast, the origination cohorts only capture shared temporal context. The inclusion of phylogenetic context as an addition individual level hierarchical

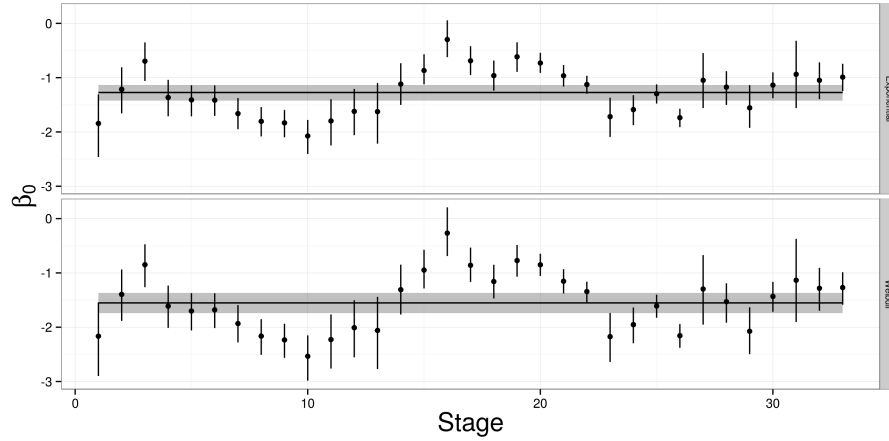


Figure 7: Comparison of cohort-specific estimates of β_0 presented along with the estimate for the overall baseline extinction risk. Points correspond to the median of the cohort-specific estimate, along with 80% credible intervals. The horizontal line is the median estimate of the overall baseline extinction risk along with 80% credible intervals. Results are presented for the exponential (top) and Weibull (bottom) models.

structure independent of origination cohort would allow for determining how

438 much of the observed variability is due to shared evolutionary history versus
actual differences associated with these taxonomic traits. For example, it has
440 been shown that phylogeny contribute non-trivially to differences in mammal
species durations SMITS IN PREP.

442 In summary, patterns of Paleozoic brachiopod survival were analyzed using a
fully Bayesian hierarchical survival modelling approach. Using a varying-slopes,
444 varying-intercepts approach I am able to model both the overall mean effect of
biological covariates on extinction risk while also modeling the correlation
446 between origination cohort-specific estimates of covariate effects. I find that as
baseline extinction risk increases, the strength of the selection gradient on
448 biological traits (except body size) increases. This manifests as greater
differences in extinction risk for each unit difference in the biological covariates

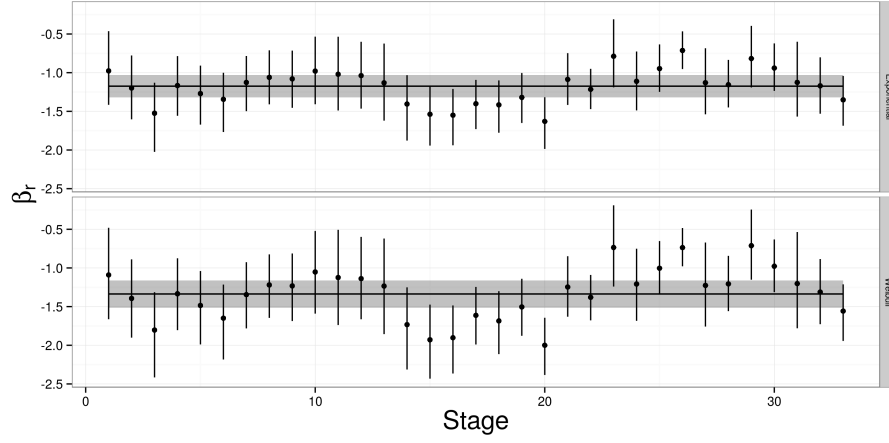


Figure 8: Comparison of cohort-specific estimates of the effect of geographic range on extinction risk β_r , presented along with the estimate for the overall effect of geographic range. Points correspond to the median of the cohort-specific estimate, along with 80% credible intervals. The horizontal line is the median estimate of the overall baseline extinction risk along with 80% credible intervals. Results are presented for the exponential (top) and Weibull (bottom) models.

450 during periods of high extinction risk, while a much flatter total selection
gradient during periods of low extinction risk. I also find some support for
452 “survival of the unspecialized” (Liow, 2004, 2007, Nürnberg and Aberhan, 2013,
2015, Simpson, 1944) as a general characterization of the effect of environmental
454 preference on extinction risk (Fig. 3), though there is heterogeneity between
origination cohorts (Fig. 9). Generally, this study demonstrates the advantages
456 of a hierarchical Bayesian framework for taking into account the structured
nature of the data. Future studies of structured data should adopt similar
458 strategies in order to best model our knowledge instead of ignoring that
structure which can lead to poor and/or incorrect inference.

460 Acknowledgements

462 I would like to thank K. Angielczyk, M. Foote, P. D. Polly, and R. Ree for
helpful discussion and advice. Additionally, thank you A. Miller for the
epicontinental versus open-ocean assignments. This entire study would would
464 not have been possible without the Herculean effort of the many contributors to
the Paleobiology Database. In particular, I would like to thank NAMES. This is
466 Paleobiology Database publication XXX.

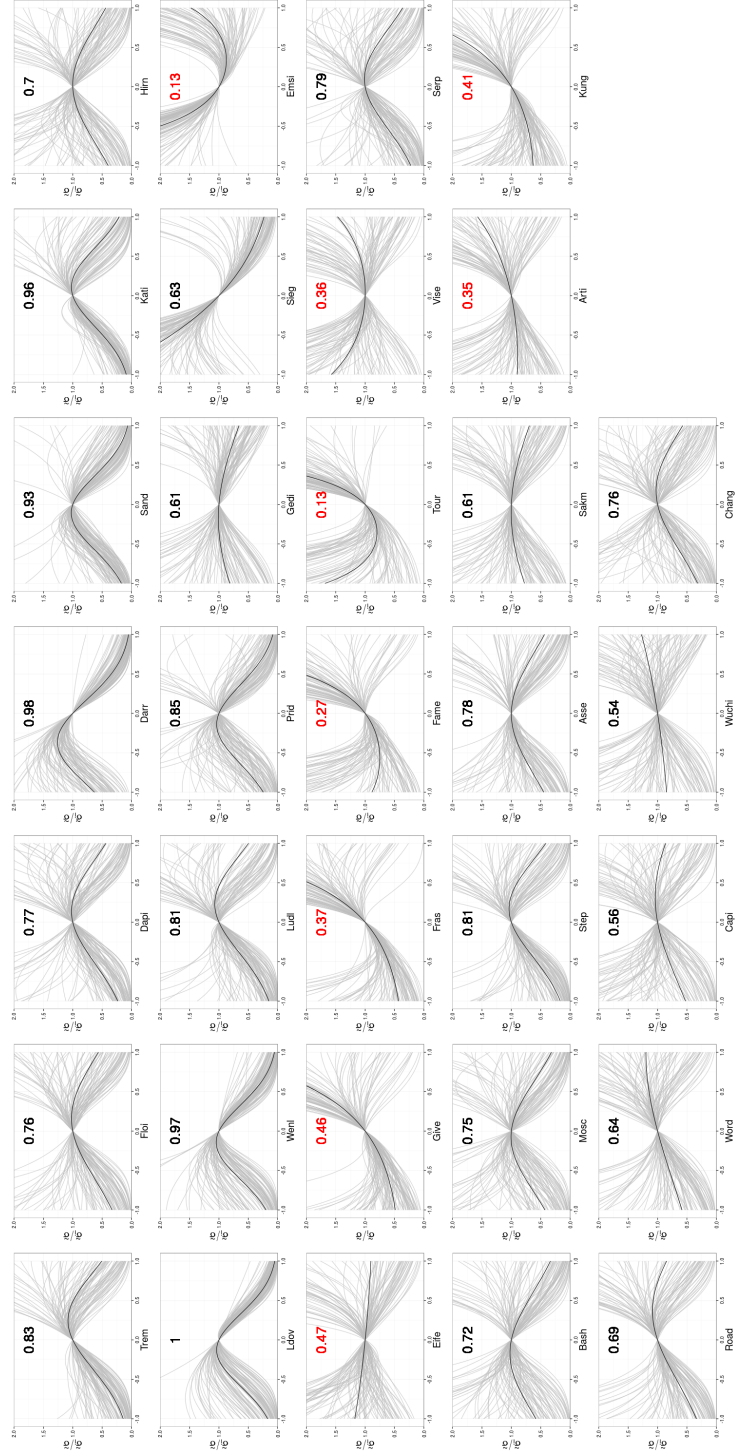


Figure 9: Comparison of the cohort-specific estimates of $f(v_i)$ (Eq. 3) for the 33 analyzed origination cohorts. The stage of origination is labeled on the x-axis of each panel. The oldest stage is in the upper left, while the youngest is in the lower left. The number in each panel corresponds to the posterior probability that $f(v_i)$ is concave down. Those that are highlighted in red have less than 51% posterior predictive probability that $f(v_i)$ is concave down.

References

- Alexander, R. R., 1977. Generic longevity of articulate brachiopods in relation to the mode of stabilization on the substrate. *Palaeogeography, Palaeoclimatology, Palaeoecology* 21:209–226.
- Baumiller, T. K., 1993. Survivorship analysis of Paleozoic Crinoidea: effect of filter morphology on evolutionary rates. *Paleobiology* 19:304–321.
- Cooper, W. S., 1984. Expected time to extinction and the concept of fundamental fitness. *Journal of Theoretical Biology* 107:603–629.
- Felsenstein, J., 1985. Phylogenies and the comparative method. *American Naturalist* 125:1–15. URL <http://www.jstor.org/stable/2461605>.
- Foote, M., 1988. Survivorship analysis of Cambrian and Ordovician Trilobites. *Paleobiology* 14:258–271.
- , 2006. Substrate affinity and diversity dynamics of Paleozoic marine animals. *Paleobiology* 32:345–366. URL <http://www.bioone.org/doi/abs/10.1666/05062.1>.
- Foote, M. and A. I. Miller, 2013. Determinants of early survival in marine animal genera. *Paleobiology* 39:171–192. URL <http://www.bioone.org/doi/abs/10.1666/12028>.
- Gelman, A., 2006. Prior distributions for variance parameters in hierarchical models. *Bayesian Analysis* 1:515–533.
- Gelman, A., J. B. Carlin, H. S. Stern, D. B. Dunson, A. Vehtari, and D. B. Rubin, 2013. *Bayesian data analysis*. 3 ed. Chapman and Hall, Boca Raton, FL.

- 490 Gelman, A. and J. Hill, 2007. Data Analysis using Regression and
Multilevel/Hierarchical Models. Cambridge University Press, New York, NY.
- 492 Hijmans, R. J., 2015. raster: Geographic data analysis and modeling. URL
<http://CRAN.R-project.org/package=raster>. R package version 2.3-24.
- 494 Hoffman, M. D. and A. Gelman, 2014. The No-U-Turn Sampler: Adaptively
Setting Path Lengths in Hamiltonian Monte Carlo. Journal of Machine
496 Learning Research 15:1351–1381.
- Housworth, E. A., P. Martins, and M. Lynch, 2004. The Phylogenetic Mixed
498 Model. The American Naturalist 163:84–96.
- Hunt, G., K. Roy, and D. Jablonski, 2005. Species-level heritability reaffirmed: a
500 comment on "On the heritability of geographic range sizes". American
Naturalist 166:129–135.
- 502 Ibrahim, J. G., M.-H. Chen, and D. Sinha, 2001. Bayesian Survival Analysis.
Springer, New York.
- 504 Jablonski, D., 1986. Background and mass extinctions: the alternation of
macroevolutionary regimes. Science 231:129–133.
- 506 ———, 1987. Heritability at the species level: analysis of geographic ranges of
cretaceous mollusks. Science 238:360–363. URL
508 <http://www.ncbi.nlm.nih.gov/pubmed/17837117>.
- Jablonski, D. and K. Roy, 2003. Geographical range and speciation in fossil and
510 living
molluscs. Proceedings. Biological sciences / The Royal Society 270:401–6. URL
512 <http://www.pubmedcentral.nih.gov/articlerender.fcgi?artid=1691247&tool=pmcentrez&rendertype>
- Johnson, J. G., 1974. Extinction of Perched Faunas. Geology 2:479–482.

- 514 Kiessling, W. and M. Aberhan, 2007. Environmental determinants of marine
benthic biodiversity dynamics through Triassic–Jurassic time. *Paleobiology*
516 33:414–434.
- Klein, J. P. and M. L. Moeschberger, 2003. *Survival Analysis: Techniques for*
518 *Censored and Truncated Data*. 2nd ed. Springer, New York.
- Liow, L. H., 2004. A test of Simpson’s “rule of the survival of the relatively
520 unspecialized” using fossil crinoids. *The American naturalist* 164:431–43.
URL <http://www.ncbi.nlm.nih.gov/pubmed/15459876>.
- 522 ———, 2007. Does versatility as measured by geographic range, bathymetric
range and morphological variability contribute to taxon longevity? *Global*
524 *Ecology and Biogeography* 16:117–128. URL
<http://doi.wiley.com/10.1111/j.1466-8238.2006.00269.x>
526 [papers2://publication/doi/10.1111/j.1466-8238.2006.00269.x](http://publication/doi/10.1111/j.1466-8238.2006.00269.x).
- Lynch, M., 1991. Methods for the analysis of comparative data in evolutionary
528 biology. *Evolution* 45:1065–1080.
- Miller, A. I. and S. R. Connolly, 2001. Substrate affinities of higher taxa and
530 the Ordovician Radiation. *Paleobiology* 27:768–778. URL
<http://www.bioone.org/doi/abs/10.1666/0094-8373%282001%29027%3C0768%3ASAOHTA%3E2.O.CO%3B2>.
- 532 Miller, A. I. and M. Foote, 2009. Epicontinental seas versus open-ocean settings:
the kinetics of mass extinction and origination. *Science* 326:1106–9. URL
534 <http://www.ncbi.nlm.nih.gov/pubmed/19965428>.
- Nürnberg, S. and M. Aberhan, 2013. Habitat breadth and geographic range
536 predict diversity dynamics in marine Mesozoic bivalves. *Paleobiology*
39:360–372. URL <http://www.bioone.org/doi/abs/10.1666/12047>.
- 538 ———, 2015. Interdependence of specialization and biodiversity in Phanerozoic

marine invertebrates. *Nature communications* 6:6602. URL
540 <http://www.ncbi.nlm.nih.gov/pubmed/25779979>.

Palmer, M. E. and M. W. Feldman, 2012. Survivability is more fundamental
542 than evolvability. *PloS one* 7:e38025. URL
<http://www.pubmedcentral.nih.gov/articlerender.fcgi?artid=3377627&tool=pmcentrez&rendertype>

544 Payne, J. L. and S. Finnegan, 2007. The effect of geographic range on
extinction risk during background and mass extinction. *Proceedings of the*
546 *National Academy of Sciences* 104:10506–11. URL
<http://www.pubmedcentral.nih.gov/articlerender.fcgi?artid=1890565&tool=pmcentrez&rendertype>

548 Payne, J. L., N. A. Heim, M. L. Knope, and C. R. McClain, 2014. Metabolic
dominance of bivalves predates brachiopod diversity decline by more than 150
550 million years. *Proceedings of the Royal Society B* 281:20133122.

Raup, D. M., 1975. Taxonomic survivorship curves and Van Valen’s Law.
552 *Paleobiology* 1:82–96. URL
<http://www.ncbi.nlm.nih.gov/pubmed/17777225>.

554 ———, 1978. Cohort Analysis of generic survivorship. *Paleobiology* 4:1–15.

Sepkoski Jr., J. J., 1981. A factor analytic description of the Phanerozoic
556 marine fossil record. *Paleobiology* 7:36–53.

Sheehan, P., 2001. The late Ordovician mass extinction. *Annual Review of*
558 *Earth and Planetary Sciences* 29:331–364. URL
<http://www.annualreviews.org/doi/abs/10.1146/annurev.earth.29.1.331>.

560 Simpson, C., 2006. Levels of selection and large-scale morphological trends.
Ph.D. thesis, University of Chicago.

562 Simpson, C. and P. G. Harnik, 2009. Assessing the role of abundance in marine

bivalve extinction over the post-Paleozoic. *Paleobiology* 35:631–647. URL
564 <http://www.bioone.org/doi/abs/10.1666/0094-8373-35.4.631>.

Simpson, G. G., 1944. *Tempo and Mode in Evolution*. Columbia University
566 Press, New York.

———, 1953. *The Major Features of Evolution*. Columbia University Press,
568 New York.

Stan Development Team, 2014a. Stan: A c++ library for probability and
570 sampling, version 2.5.0. URL <http://mc-stan.org/>.

———, 2014b. *Stan Modeling Language Users Guide and Reference Manual*,
572 Version 2.5.0. URL <http://mc-stan.org/>.

Van Valen, L., 1973. A new evolutionary law. *Evolutionary Theory* 1:1–30.
574 URL <http://ci.nii.ac.jp/naid/10011264287/>.

———, 1979. Taxonomic survivorship curves. *Evolutionary Theory* 4:129–142.

576 Wang, S. C., 2003. On the continuity of background and mass extinction.
Paleobiology 29:455–467. URL
578 <http://www.bioone.org/doi/abs/10.1666/0094-8373%282003%29029%3C0455%3AOTCOBA%3E2.0.CO%3B2>.

Watanabe, S., 2010. Asymptotic Equivalence of Bayes Cross Validation and
580 Widely Applicable Information Criterion in Singular Learning Theory.
Journal of Machine Learning Research 11:3571–3594.

582 A Uncertainty in environmental preference

The calculation and inclusion of environmental affinity in the survival model is a
584 statistical procedure that takes into account our uncertainty based on where
fossils tend to occur. Because we cannot directly observe if a fossil taxon had
586 occurrences restricted to only a single environment, instead we can only
estimate its affinity with uncertainty. One advantage of using a Bayesian
588 analytical approach is that both parameters and data are considered random
samples from some underlying distribution, which means that it is possible to
590 model the uncertainty in our covariates of interest (Gelman et al., 2013). My
approach is conceptually similar to Simpson and Harnik (2009) but instead of
592 obtaining a single point estimate, an entire posterior distribution is estimated.

The first step is to determine the probability θ at which genus i occurs in an
594 epicontinental settings based on its own pattern of occurrences. Define e_i as the
number of occurrences of genus i in an epicontinental sea and o_i as the number of
596 occurrences of genus i not in an epicontinental sea (e.g. open ocean). Because
the value of interest is the probability of occurring in an epicontinental
598 environment, given the observed fossil record, I assume that probability follows
a binomial distribution. We can then define our sampling statement as

$$e_i \sim \text{Binomial}(e_i + o_i, \theta_i). \quad (4)$$

600 I used a flat prior for θ_i defined as $\theta_i \sim \text{Beta}(1, 1)$. Because the beta
distribution is the conjugate prior for the binomial distribution, the posterior is
602 easy to compute in closed form. The posterior probability of θ is then

$$\theta_i \sim \text{Beta}(e_i + 1, o_i + 1) \quad (5)$$

It is extremely important, however, to take into account the overall
604 environmental occurrence probability of all other genera present at the same
time as genus i . This is incorporated as an additional probability Θ . Define E_i
606 as the total number of other fossil occurrences (except for genus i) in
epicontinental seas during stages where i occurs and O_i as the number of other
608 fossil occurrences not on epicontinental seas. We can then define the sampling
statement as

$$E_i \sim \text{Binomial}(E_i + O_i, \Theta_i). \quad (6)$$

610 Again, I used a flat prior of Θ_i defined as $\Theta_i \sim \text{Beta}(1, 1)$. The posterior of Θ is
then simply defined as

$$\Theta_i \sim \text{Beta}(E_i + 1, O_i + 1) \quad (7)$$

612 I then define the environmental affinity of genus i as $v_i = \theta_i - \Theta_i$. v_i is a value
that can range between -1 and 1, where negative values indicate that genus i
614 tends to occur more frequently in open ocean environments than background
while positive values indicate that genus i tends to occur in epicontinental
616 environments.

While this approach is noticeably more complicated than previous ones (Foote,
618 2006, Kiessling and Aberhan, 2007, Miller and Connolly, 2001, Simpson and
Harnik, 2009) there are some important benefits to both using a continuous
620 measure of affinity as well directly modeling our uncertainty. In order to show
some of these benefits, I performed a simulation analysis of how
622 modal/maximum *a posteriori* (MAP) estimates versus full posterior estimates.

In this simulation, I first defined the “background” epicontinental occurrence θ_b
624 as 0.50 with a small amount of noise. This was represented as a beta distribution

$$\Theta_b = \text{Beta}(\alpha = 2500, \beta = 2500). \quad (8)$$

This choice of parameters for the distribution reflects the average number of
626 background occurrences for either epicontinental or open ocean environments
per genus.

628 Using this background occurrence ratio, I randomly generated the occurrence
patterns of 1000 simulated taxa. This was done at multiple sample sizes (1, 2, 3,
630 4, 5, 10, 25, 50, 100) in order to demonstrate the effects of increasing sample
size on the confidence of environmental affinity. For each simulated taxon I
632 calculated the full posterior distribution while assuming a flat Beta prior
(Beta(1, 1)). Using the full posterior I calculated the MAP probability of
634 occurring in epicontinental environments. The environmental affinity was
calculated for each of the simulated taxa using both the full posterior and the
636 MAP estimate. In this toy example, environmental affinity can range between
-0.5 and 0.5.

638 As should be expected, as sample size increases the distribution of MAP
estimates converge on the true value (Fig. 10). For taxa with less than 10
640 occurrences, the MAP estimate is biased towards extreme values. Note that the
mode of the beta distribution is not defined for situations where there were 0
642 draws of one of the environmental conditions. Instead, the vertical line is based
entirely on the observed occurrences which are technically the modal estimates
644 because they are the most frequently occurring/highest density.

In contrast, we can compare the true occurrence probability distribution versus
646 the posterior estimate for a given sample (Fig. 11). When sample sizes are low,
posterior estimates are flat and represent a compromise between the likelihood
648 and the flat prior (Eq. 5). Because of this, estimates from small sizes are less

likely to be overly biased towards the extremes. This is further emphasized by
650 inspection of the estimates of environmental affinity for the simulated taxa (Fig.
12). Posterior estimates from simulated taxa with small sample size have a
652 much broader distribution that both allows for the extreme observation but still
captures the “true” value (0).

654 By defining environmental preference as the difference in full posterior estimates
of occurrence probability, it is possible to include taxa with low sample sizes
656 that are normal discarded (Foote, 2006, Kiessling and Aberhan, 2007, Miller
and Connolly, 2001, Simpson and Harnik, 2009). Additionally, 55+% of
658 observed Paleozoic brachiopod genera have less than 10 occurrences which is the
range of sample sizes where MAP (or ML) estimates would be potentially most
660 biased. This is preferable to finding the difference between the MAP estimates
(blue line; Fig. 12).

662 B Survival model

The simplest model of genus duration includes no covariate or structural
664 information. Define y_i as the duration in stages of genus i , where $i = 1, \dots, n$
and n is the number of observed genera. These two models are then simply
666 defined as

$$\begin{aligned} y_i &\sim \text{Exponential}(\lambda) \\ y_i &\sim \text{Weibull}(\alpha, \sigma). \end{aligned} \tag{9}$$

λ, α , and σ are all defined for all positive reals. Note that λ is a “rate” or
668 inverse-scale while σ is a scale parameter, meaning that $\frac{1}{\lambda} = \sigma$.

These simple models can then be expanded to include covariate information as
670 predictors by reparameterizing λ or σ as a regression (Klein and Moeschberger,

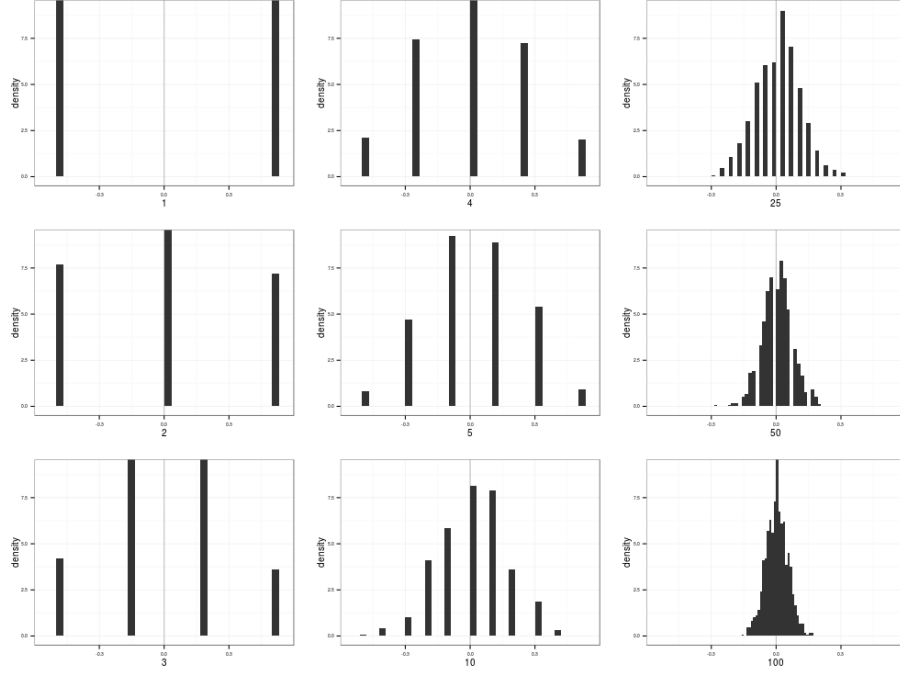


Figure 10: Histograms of the distributions of from the beta distribution defined in Eq. 8. As to be expected, as sample size increases the draws better resemble the underlying true distribution. Sample size is indicated as the label of the x-axis, increasing in column major order.

2003). Each of the covariates of interest is given its own regression coefficient
 672 (e.g. β_r) along with an intercept term β_0 . There are some additional
 complications to the parameterization of σ associated with the inclusion of α as
 674 well as for interpretability (Klein and Moeschberger, 2003). Both of these are
 then written as

$$\begin{aligned}\lambda_i &= \exp(\beta_0 + \beta_r r_i + \beta_v v_i + \beta_{v^2} v_i^2 + \beta_m m_i) \\ \sigma_i &= \exp\left(\frac{-(\beta_0 + \beta_r r_i + \beta_v v_i + \beta_{v^2} v_i^2 + \beta_m m_i)}{\alpha}\right).\end{aligned}\tag{10}$$

676 The quadratic term for environmental affinity v is to allow for the possible
 nonlinear relationship between environmental affinity and extinction risk.

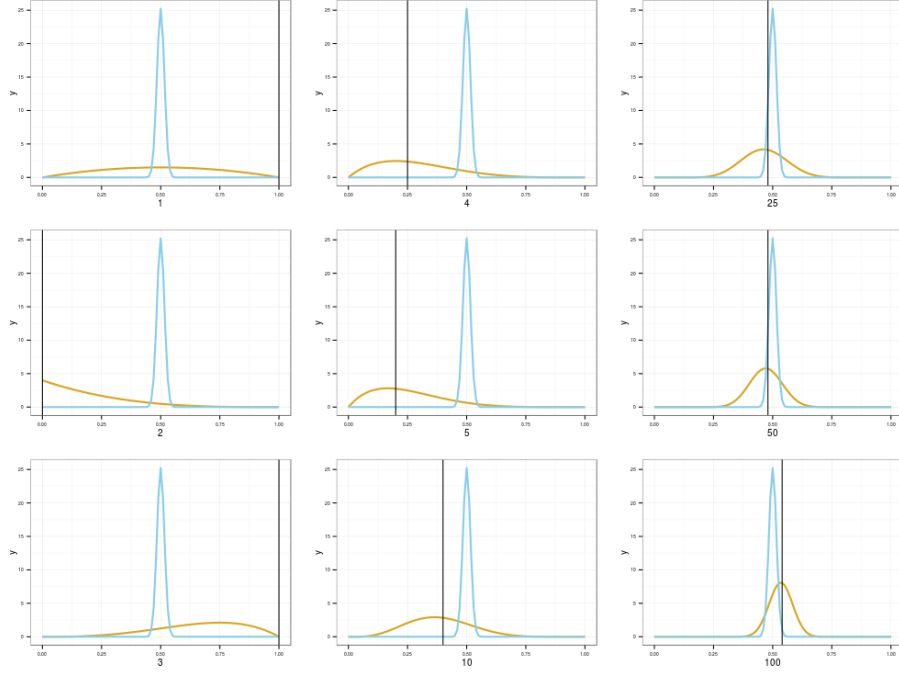


Figure 11: Comparisons of the underlying distribution (blue) to posterior estimates based on increasing sample size (gold). Each posterior estimate is represented for only a single realization of draws, each with sample size indicated as the x-axis label (increasing in column major order). Black vertical lines correspond to the MAP estimate of the simulated taxon’s affinity. This stands in contrast to the posterior distribution of expected affinity in gold.

678 The models which incorporate both equations 9 and 10 can then be further
expanded to allow all of the β coefficients, including β_0 , to vary with origination
680 cohort while also modeling their covariance and correlation. This is called a
varying-intercepts, varying-slopes model (Gelman and Hill, 2007). It is much
682 easier to represent and explain how this is parameterized using matrix notation.
First, define \mathbf{B} as $k \times J$ matrix of the k coefficients including the intercept term
684 ($k = 5$) for each of the J cohorts. Second, define \mathbf{X} as a $n \times k$ matrix where each
column is one of the covariates of interest. Importantly, \mathbf{X} includes a columns of
686 all 1s which correspond to the constant term β_0 . Third, define $j[i]$ as the

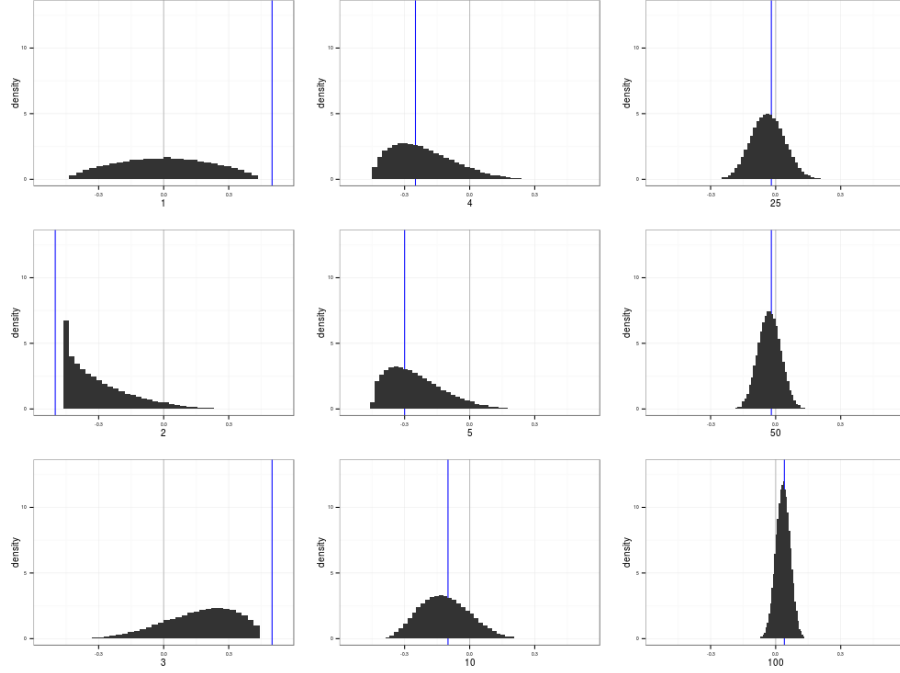


Figure 12: Histograms of the difference in the underlying occurrence distribution and the posterior distribution estimates from the previous graph (Fig. 11). The “true” value is included in all distributions of environmental affinities. Each affinity estimate is represented for only a single realization of draws, each with sample size indicated as the x-axis label (increasing in column major order). Blue vertical lines correspond to the difference in MAP estimates between the underlying distribution and the simulated taxon’s draws. This stands in contrast to the distribution of the differences between the simulated taxon and background.

origination cohort of genus i , where $j = 1, \dots, J$ and J is the total number of
688 observed cohorts. We then rewrite λ and σ of equation 10 in matrix notation as

$$\begin{aligned}\lambda_i &= \exp(\mathbf{X}_i B_{j[i]}) \\ \sigma_i &= \exp\left(\frac{-(\mathbf{X}_i B_{j[i]})}{\alpha}\right).\end{aligned}\tag{11}$$

Because B is a matrix, I use a multivariate normal prior with unknown vector

690 of means μ and covariance matrix Σ . This is written as

$$B \sim \text{MVN}(\vec{\mu}, \Sigma) \quad (12)$$

where $\vec{\mu}$ is length k vector representing the overall mean of the distributions of
692 β coefficients. Σ is a $k \times k$ covariance matrix of the β coefficients.

What remains is assigning priors the elements of $\vec{\mu}$ and the covariance matrix Σ .
694 All elements of $\vec{\mu}$ except for μ_r were given weakly informative normal priors
while μ_r was given an informative normal prior ($\mu_r \sim \mathcal{N}(-1, 1)$). The prior for Σ
696 is a bit more complicated due to its multivariate nature. Following the Stan
Development Team (2014b), I modeled the scale terms separate from the
698 correlation structure of the coefficients. This is possible because of the
relationship between a covariance and a correlation matrix, defined as

$$\Sigma_B = \text{Diag}(\vec{\tau})\Omega\text{Diag}(\vec{\tau}) \quad (13)$$

700 where $\vec{\tau}$ is a length k vector of variances and $\text{Diag}(\tau)$ is a diagonal matrix.

I used a LKJ prior distribution for correlation matrix Ω as recommended by
702 Stan Development Team (2014b). The LKJ distribution is a single parameter
multivariate distribution where values of the parameter η greater than 1
704 concentrate density at the unit correlation matrix, which corresponds to no
correlation between the β coefficients. The scale parameters, $\vec{\tau}$, are given weakly
706 informative half-Cauchy (C^+) priors following Gelman (2006).

C Censored observations

708 A key aspect of survival analysis is the inclusion of censored, or incompletely
observed, data points (Ibrahim et al., 2001, Klein and Moeschberger, 2003). The
710 two classes of censored observations encountered in this study were right and
left censored observations. Right censored genera are those that did not go
712 extinct during the window of observation, or genera that are still extant. Left
censored observations are those taxa for which we know only an upper limit on
714 their duration.

In the context of this study, I considered all genera that had a duration of only
716 one geologic stage to be left censored as we do not have a finer degree of
resolution.

718 The key function for modeling censored observations is the survival function, or
 $S(t)$. $S(t)$ corresponds to the probability that a genus having existed for t stages
720 will not have gone extinct while $h(t)$ corresponds to the instantaneous
extinction rate at taxon age t Klein and Moeschberger (2003). For an
722 exponential model, $S(t)$ is defined as

$$S(t) = \exp(-\lambda t), \quad (14)$$

and for the Weibull distribution $S(t)$ is defined as

$$S(t) = \exp\left(-\left(\frac{t}{\sigma}\right)^\alpha\right). \quad (15)$$

724 $S(t)$ is equivalent to the complementary cumulative distribution function,
 $1 - F(t)$ (Klein and Moeschberger, 2003).

726 For right censored observations, instead of calculating the likelihood as normal

(Eq. 11) the likelihood of an observation is evaluated using $S(t)$. Conceptually,
 728 this approach calculates the likelihood of observing a taxon that existed for at
 least that long. For left censored data, instead the likelihood is calculated using
 730 $1 - S(t)$ which corresponds to the likelihood of observing a taxon that existed
 no longer than t .

732 The full likelihood statements incorporating fully observed, right censored, and
 left censored observations are then

$$\begin{aligned}\mathcal{L} &\propto \prod_{i \in C} \text{Exponential}(y_i | \lambda) \prod_{j \in R} S(y_j | \lambda) \prod_{k \in L} (1 - S(y_k | \lambda)) \\ \mathcal{L} &\propto \prod_{i \in C} \text{Weibull}(y_i | \alpha, \sigma) \prod_{j \in R} S(y_j | \alpha, \sigma) \prod_{k \in L} (1 - S(y_k | \alpha, \sigma))\end{aligned}\tag{16}$$

734 where C is the set of all fully observed taxa, R the set of all right censored taxa,
 and L the set of all left-censored taxa.

736 D Widely applicable information criterion

WAIC can be considered a fully Bayesian alternative to the Akaike information
 738 criterion, where WAIC acts as an approximation of leave-one-out
 cross-validation which acts as a measure of out-of-sample predictive accuracy
 740 (Gelman et al., 2013). WAIC is calculated starting with the log pointwise
 posterior predictive density calculated as

$$\text{lppd} = \sum_{i=1}^n \log \left(\frac{1}{S} \sum_{s=1}^S p(y_i | \Theta^s) \right), \tag{17}$$

742 where n is sample size, S is the number posterior simulation draws, and Θ
 represents all of the estimated parameters of the model. This is similar to
 744 calculating the likelihood of each observation given the entire posterior. A

correction for the effective number of parameters is then added to lppd to
746 adjust for overfitting. The effective number of parameters is calculated,
following the recommendations of Gelman et al. (2013), as

$$p_{\text{WAIC}} = \sum_{i=1}^n V_{s=1}^S (\log p(y_i | \Theta^S)). \quad (18)$$

748 where V is the sample posterior variance of the log predictive density for each
data point.

750 Given both equations 17 and 18, WAIC is then calculated

$$\text{WAIC} = \text{lppd} - p_{\text{WAIC}}. \quad (19)$$

When comparing two or more models, lower WAIC values indicate better
752 out-of-sample predictive accuracy. Importantly, WAIC is just one way of
comparing models. When combined with posterior predictive checks it is
754 possible to get a more complete understanding of a model's fit to the data.